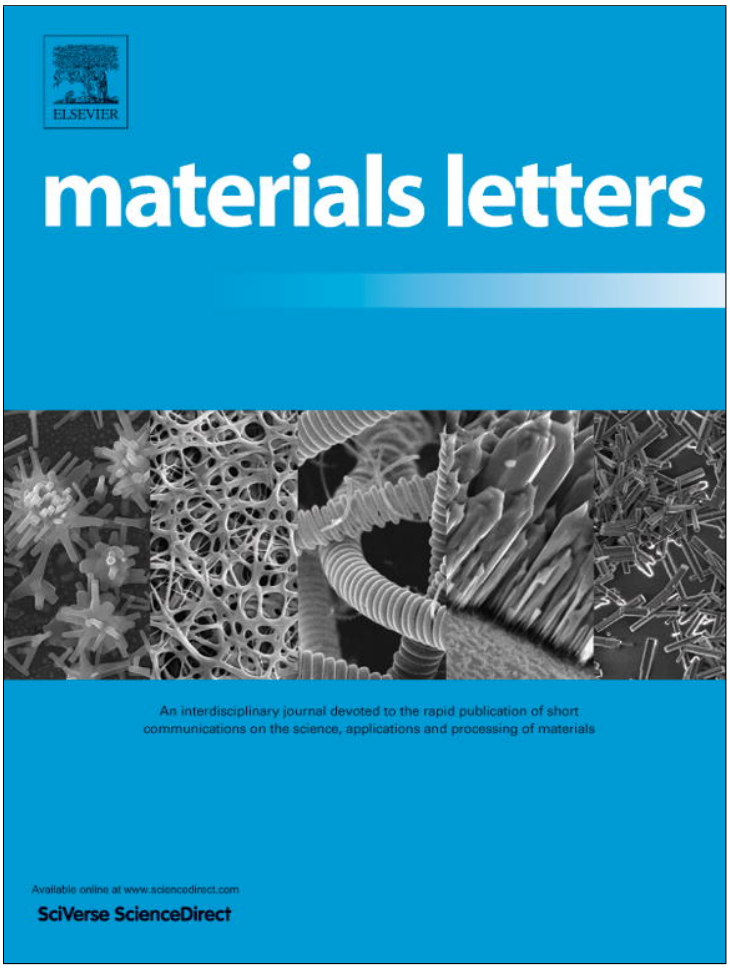

(This is a sample cover image for this issue. The actual cover is not yet available at this time.)

Materials Letters 81 (2012) 225–228

Contents lists available at SciVerse ScienceDirect

Materials Letters

journal homepage: www.elsevier.com/locate/matlet

Phase transformations in the severely plastically deformed Zr–Nb alloys

B.B. Straumal [a,b,*], A.S. Gornakova [a], A.A. Mazilkin [a,b], O.B. Fabrichnaya [c], M.J. Kriegel [c], B. Baretzky [b], J.-Z. Jiang [d], S.V. Dobatkin [e]

[a] Institute of Solid State Physics RAS, 142432 Chernogolovka, Russia
[b] Karlsruher Institut für Technologie, Institut für Nanotechnologie, Hermann-von-Helmholtz-Platz 1, 76344 Eggenstein-Leopoldshafen, Germany
[c] TU Bergakademie Freiberg, Institut für Werkstoffwissenschaft, 09599 Freiberg, Germany
[d] Department of Materials Science and Engineering, Zhejiang University, 310027 Hangzhou, China
[e] Institute of Metallurgy and Materials Science RAS, 117991 Moscow, Russia

ARTICLE INFO

Article history:
Received 22 April 2012
Accepted 29 April 2012
Available online 9 May 2012

Keywords:
Nanocrystalline materials
High pressure torsion
Phase transitions
Zr–Nb alloys
Cladding of nuclear fuel

ABSTRACT

Zr–Nb alloys play the important role in the energy production of being the main material for the cladding of nuclear fuel in the nuclear power plants. Severe plastic deformation by high-pressure torsion (HPT) leads to the strong grain refinement in Zr–Nb alloys. HPT leads also to formation of the high-pressure ωZr phase. It remains quenched at the ambient pressure and disappears by heating only above 400 °C. The diffusion-controlled αZr + βNb↔αZr + βZr↔βZr transformations are observed only in the as-cast alloy Zr–2.5 mass% Nb. Transformation αZr↔βZr in as-cast alloy Zr–8 mass% Nb occurs as martensitic. Phase transformations occurring in alloys of both compositions after HPT on heating are martensitic. The effective temperature during HPT has been determined as T_{eff} = 700 °C at 5 GPa.

1. Introduction

Zr–Nb alloys play the important role in the energy production of being the main material for the cladding of nuclear fuel in the nuclear power plants [1,2]. Severe plastic deformation (SPD) permits to obtain the extremely fine-grained structure in Zr and Zr alloys [3–5 and references therein]. They contain also the high pressure ω-phase which remains quenched after the release of high pressure. If one compares the phases in alloys before and after SPD with an equilibrium phase diagram, one can estimate the effective temperature during SPD treatment [6]. The investigation of peculiarities of phase transformations in the SPD-treated Zr–Nb alloys was the goal of this work.

2. Experimental

Two Zr–Nb alloys with 2.5 and 8 wt.% Nb were melted in a vacuum with high purity components (4 N Zr and 4 N Nb). The cast disks of 0.7 mm thick were deformed by high-pressure torsion (HPT) at 5 GPa (5 torsions, 1 rotation-per-minute). X-ray diffraction (XRD) data were obtained on a Siemens diffractometer (Co K_α radiation). Grain size was estimated by XRD line broadening using the Scherer formula [7]. Both the as-cast and fine-grained HPT-samples were studied by differential scanning calorimetry (DSC) in the temperature range of 100–900 °C using the NETZSCH Pegasus 404C calorimeter in the dry argon atmosphere, in Al_2O_3 crucibles and at the cooling and heating rates of 20 K/min. Thermodynamic calculations were performed using the thermodynamic data of Guillermet [8] where solid solutions with bcc and hcp (αZr) structures as well as liquid solution were described by using a substitutional model. The bcc phase is described as single phase which forms miscibility gap βZr + βNb in the composition range from 8 to 81 wt.% Zr and temperatures from 620 up to 976 °C. Thermo-calc software [9] was used to calculated equilibrium phase diagrams and diffusionless transformation αZr↔βZr.

3. Results and discussion

The grain size in both as-cast alloys was about 500–800 μm [10]. HPT drastically refined the grains. Grain size after HPT was only about 20 nm. XRD-spectra of as-cast alloys (Fig. 1a) demonstrate that they contain mainly αZr with hexagonal closely-packed (hcp) lattice. The Nb-rich body-centered cubic (bcc) phase (βNb in Fig. 2) is absent. Small amount of βZr is present in the as-cast alloys. Zr-rich βZr has a body-centered cubic lattice and is isomorhous to the Nb-rich phase (βNb). The calculated phase diagram (Fig. 2a) reproduces experimental data [11] very well. Below the temperature of a monotectoid transformation T_{mon} = 620 °C the stable assemblage is βNb + αZr according to the Zr–Nb phase diagram (Fig. 2a). Above monotectoid reaction at composition Zr > 81 mass% βZr is in equilibrium with αZr phase which transforms into βZr single phase with temperature increase. For compositions with Zr content between 8 and 81 wt.% and temperatures between monotectoid reaction and critical point T_c = 976 °C there is a two-phase area βNb + βZr

* Corresponding author at: Institute of Solid State Physics RAS, 142432 Chernogolovka, Russia. Tel./fax: +7 499 2382326.
E-mail address: straumal@issp.ac.ru (B.B. Straumal).

0167-577X/$ – see front matter © 2012 Elsevier B.V. All rights reserved.
doi:10.1016/j.matlet.2012.04.153

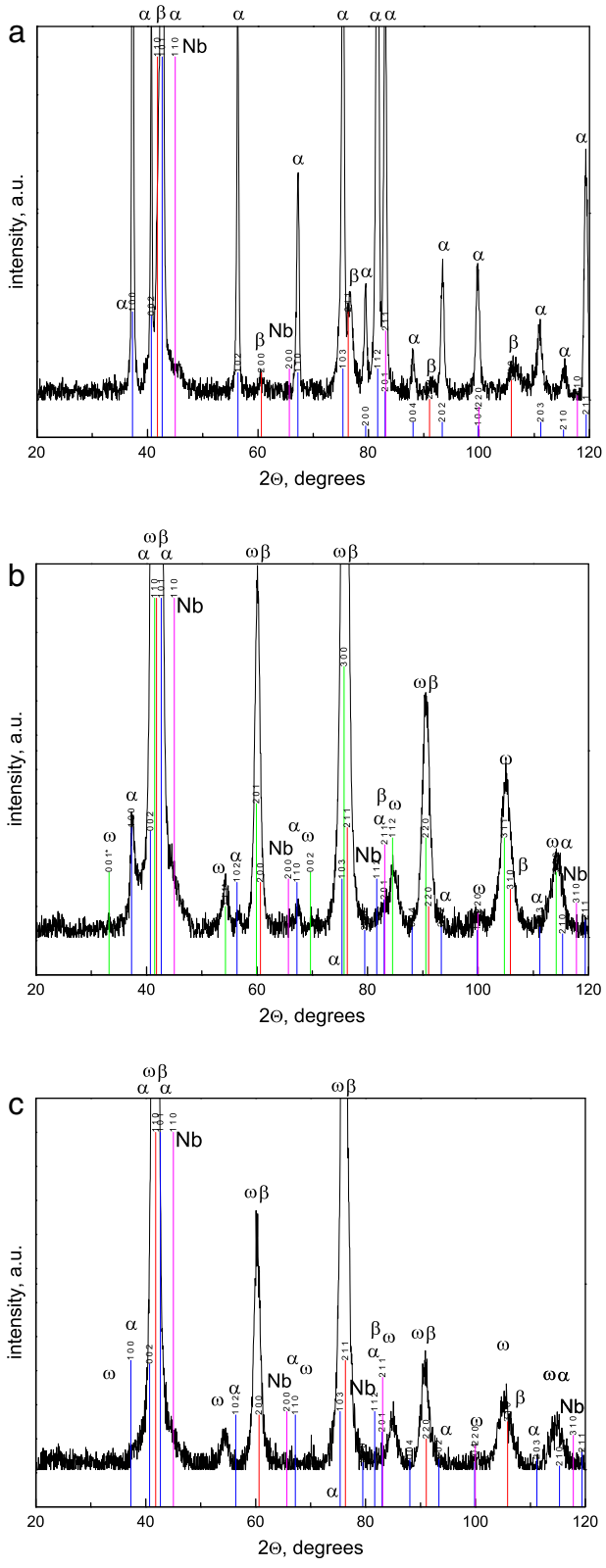

Fig. 1. XRD curves for the (a) as-cast CG Zr–2.5 wt.% Nb alloy, (b) UFG Zr–2.5 wt.% Nb alloy after HPT and (c) UFG Zr–8 wt.% Nb alloy after HPT.

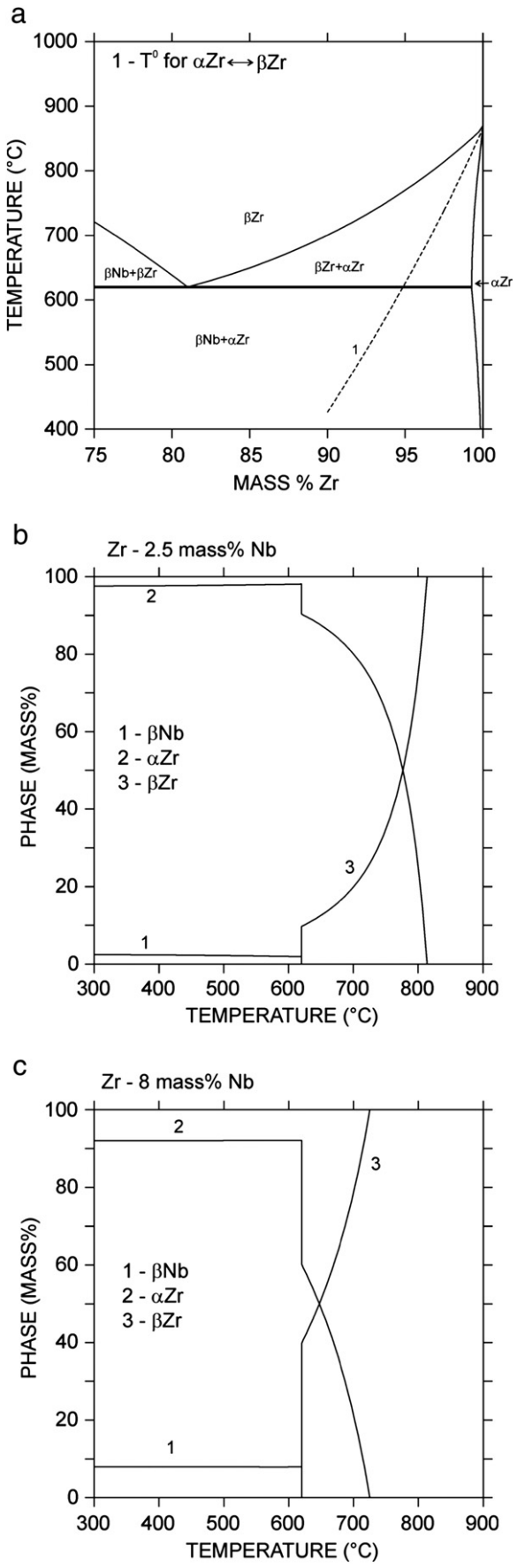

Fig. 2. (a) The part of the Zr–Nb phase diagram and temperature dependence of the equilibrium amount of βNb, αZr and βZr phases forming the (b) Zr–2.5 wt.% Nb and (c) Zr–8 wt.% Nb alloys calculated using the THERMO-CALC program. Dashed line in (a) shows the martensitic αZr→βZr transformation.

(Fig. 2a). After HPT both fine-grained Zr–Nb alloys contain mainly the ωZr phase (Fig. 1b,c) with hexagonal C32 structure [12]. At the diffraction angle 2Θ = 54° the peak of a ωZr (C32) phase is clearly visible without overlapping with peaks of other phases. αZr (hcp-phase) almost disappeared after HPT. The Nb-rich bcc phase (βNb) is absent both after and before HPT. All diffraction peaks of the βZr phase are very close to the peaks of ωZr phase. Nevertheless, the positions of peaks at 2Θ = 60°, 76°, 91 and 105° for the Zr–2.5 wt.% Nb alloy after HPT (Fig. 1b) almost perfectly coincide with the tabulated values for 201, 300, 220 and 311 peaks for the ωZr phase. In the Zr–2.5 wt.% Nb alloy the same diffraction peaks are shifted to the right and are positioned between the respective tabulated values for the ωZr and βZr phases. In other words, the amount of βZr phase after HPT is much higher in the Zr–2.5 wt.% Nb alloy than in the Zr–8 wt.% Nb one.

In Fig. 3 the temperature dependences of heat flow (DSC curves) and its time derivative DDSC are shown for the as-cast and HPT-treated Zr–Nb alloys. In the as-cast Zr–2.5 wt.% Nb alloy (Fig. 3a) three heat effects are clearly visible. The onset at 505 °C can be due to the transformation of retained βZr which was found in as-cast alloys (Fig. 1a) into equilibrium assemblage βNb + αZr. The second one is due to monotectoid reaction αZr + βNb↔βZr (onset at 623.1 °C) and the third one is due to change of the αZr + βZr two-phase area into single βZr phase around 746 °C (onset) showing deep minimum at 815 °C. These temperatures (623 and 815 °C) agree with the respective ones in the equilibrium Zr–Nb phase diagram (Fig. 2). During cooling the transformation of βZr into βZr + αZr assemblage was observed at slightly lower temperature (~790 °C). These results agree with the data of Stewart et al. [13], who showed that Zr alloys with 3.05 wt.% Nb transforms into αZr + βZr and βZr single phase by nucleation and growth mechanism at cooling rates below 10 K/s. The DSC curve for the as-cast Zr–8 wt.% Nb alloy looks different (Fig. 3b). The non-equilibrium phase βZr found in as-cast Zr–8 wt.% Nb alloy transforms into αZr phase at 445 °C, which transforms into βZr at 511 °C by diffusionless mechanism. This is in agreement with calculated αZr↔βZr transformation shown by a dashed line in Fig. 2a. At further heating martensite βZr continuously transforms into equilibrium assemblage αZr + βZr which finally transforms into stable βZr at 730 °C corresponding to deep minimum at DSC curve. The curves for the HPT-treated samples are presented in Fig. 3c–d. Reaction with a very pronounced heat effect starts at 492.2 °C in the Zr–2.5 wt.% Nb alloy and at 459.3 °C in the Zr–8 wt.% Nb alloy. Heat effects at these temperatures were not observed if the HPT-treated samples were heated again after the first DSC-run. Therefore, they can be attributed with transformation of metastable ωZr into αZr phase. These results are also in agreement with the temperature of ωZr formation during fast cooling at 400–450 °C [13]. The difference between DCS curves in the first and second runs are definitely influenced also by the (inevitable) grain growth in the HPT-treated alloy [14,15]. The heat effect of the recrystallization of nanograined SPD-treated alloys during diffusion anneals has been analyzed recently in Ref. [14]. The grain growth heat releases during first DSC run and does not appear during the second one. It has to be underlined that the amount of ωZr was lower in the Zr–8 wt.% Nb alloy and that it transformed to αZr phase at lower temperature. The second feature in alloy Zr–2.5 wt.% Nb at 568.4 °C can be explained by the transformation of metastable βZr found in HPT treated alloy into αZr phase. The second heat effect for Zr–8 wt.% Nb alloy at 519 °C can be explained by diffusionless transformation of αZr to βZr which is in agreement with calculated temperature αZr↔βZr (503 °C). It should be mentioned that all transformations at temperatures below 620 °C occur by diffusionless mechanism. It is known that the α↔β transition in Zr and Ti alloys can proceed as diffusionless martensitic one [16,17]. The martensite αZr in Zr–2.5 wt.% Nb alloy at temperatures above monotectoid reaction was continuously transforming into equilibrium αZr + βZr assemblage up to formation of single βZr phase. This transformation corresponds to the deep minima in DSC curves at 750 °C. Martensite βZr in the Zr–8 wt.% Nb alloy was continuously transforming into equilibrium αZr + βZr assemblage up to formation of βZr at 710 °C. The grain size effect on the presence or absence of martensitic

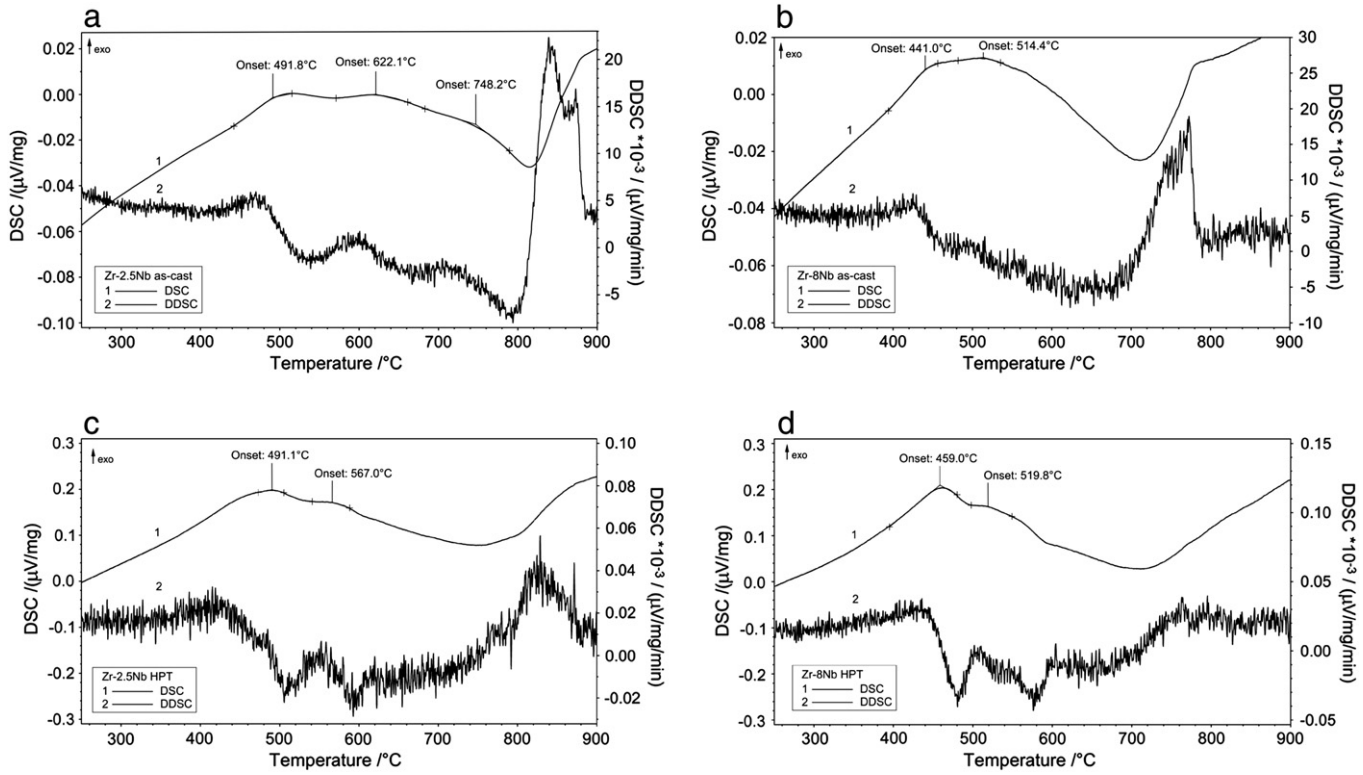

Fig. 3. The temperature dependences of heat flow DSC (upper curves) and its time derivative DDSC (lower curves) for (a) as-cast Zr–2.5 wt.% Nb alloy, (b) as-cast Zr–8 wt.% Nb alloy, (b) UFG Zr–2.5 wt.% Nb alloy after HPT and (c) UFG Zr–8 wt.% Nb alloy after HPT.

transformation has been observed in precipitates in Zr–1 wt.% Nb alloy [17]. Therefore, we can suppose that the clear change from diffusional to martensitic transformations in the HPT-treated Zr–Nb alloys in comparison with as-cast alloys could be due to the SPD-driven grain refinement.

Usually, the high pressure decreases the diffusivity and grain boundary mobility [18,19]. However, the atom movements caused by strong external forces can drive both accelerated diffusion and phase transformations in the material [10]. Following the idea proposed for the materials under severe irradiation [20], we suppose that the forced mixing emulates the increase of entropy and changes the thermodynamic potentials in the alloy. As a result, the phases forming during SPD do not correspond to the equilibrium at the treatment temperature. One can find them in an equilibrium phase diagram at a higher temperature called effective temperature T_{eff}. The HPT-treatment in our work at 5 GPa allowed the formation of the ωZr high-pressure allotrope. The ωZr phase became stable at room temperature above 3.4 GPa [21] and remained in our samples also at ambient pressure after SPD-treatment. Such phenomenon has been observed both in Zr- and Ti-based alloys but not in Hf [3–5 and references therein]. Therefore, in order to determine T_{eff} one has to use the equilibrium phase diagram at high pressures. The mixture of ωZr and βZr phases in the absence of αZr is present at 5 GPa in the narrow interval between 680 and 720 °C [22]. Therefore, in our case T_{eff} = 700 °C.

4. Conclusions

(1) Severe plastic deformation by HPT leads to the strong grain refinement in Zr–Nb alloys; (2) the high-pressure ωZr phase appears during HPT and remains quenched in both studied alloys at the ambient pressure; (3) ωZr phase disappears by heating only between 400 and 500 °C; (4) the αZr + βNb↔αZr + βZr↔βZr transformations are diffusion-controlled in the as-cast alloy Zr–2.5 mass% Nb while transformation αZr↔βZr in the as-cast alloy Zr–8 mass% Nb is martensitic. The transformations of ωZr in both ultra-fine-grained alloys after HPT-treatment occur by diffusionless mechanism. The effective temperature during HPT has been determined as T_{eff} = 700 °C.

Acknowledgment

The authors thank the Russian Foundation for Basic Research (grants 11-02-92694, 11-08-90439, and 10-02-00086) for the financial support.

References

[1] Beskorovainyi NM, Kalin BA, Platonov PA, Chernov II. Structural materials for nuclear reactors. Moscow: Energoatomisdat; 1995 (in Russian).
[2] Zuev LB, Semukhin BS, Zavodchikov SY. Mater Lett 2005;57:1015–20.
[3] Zhilyaev AP, Sabirov I, González-Doncela G, Molina-Aldareguía J, Srinivasarao B, Pérez-Prado MT. Mater Sci Eng A 2011;528:3496–505.
[4] Edalati K, Matsubara E, Horita Z. Metall Mater Trans A 2009;40:2079–86.
[5] Edalati K, Horita Z, Mine Y. Mater Sci Eng A 2010;527:2136–41.
[6] Straumal BB, Mazilkin AA, Baretzky B, Rabkin E, Valiev RZ. Mater Trans 2012;53:63–71.
[7] Ungar T, Borbely A. Appl Phys Lett 1996;69:3173–5.
[8] Guillermet AF. Z Metallkd 1991;82:478–87.
[9] Andresson J-O, Helander T, Höglund L, Shi P, Sundman B. Calphad 2002;26:273–312.
[10] Straumal BB, Gornakova AS, Kucheev YO, Baretzky B, Nekrasov AN. J Mater Eng Perform 2012;21, doi:10.1007/s11665-012-0158-7.
[11] Massalski TB, editor. Binary alloy phase diagrams. 2nd ed. Materials Park, OH: ASM International; 1990.
[12] Sikka SK, Vohra YK, Chidambaram R. Prog Mater Sci 1982;27:245–310.
[13] Stewart D, Hatt BA, Roberts JA. Br J Appl Phys 1965;16:1081–8.
[14] Amouyal Y, Divinski SV, Klinger L, Rabkin E. Acta Mater 2008;56:5500–13.
[15] Straumal BB, Kogtenkova OA, Protasova SG, Zięba P, Czeppe T, Baretzky B, et al. J Mater Sci 2011;46:4243–7.
[16] Davis R, Flower HM, West DRF. J Mater Sci 1975;14:712–22.
[17] Neogy S, Krishna KVM, Srivastava D, Dey GK. Philos Mag 2011;91:4447–64.
[18] Kedves FJ, Erdélyi G. Def Diff Forum 1989;66–69:175–88.
[19] Molodov DA, Straumal BB, Shvindlerman LS. Scr Metall 1984;18:207–11.
[20] Martin G. Phys Rev B 1984;30:1424–36.
[21] Zhang J, Zhao Y, Pantea C, Qian J, Rigg P, Hixson R, et al. J Phys Chem Solids 2005;66:1213–9.
[22] Zhang J, Zhao Y, Rigg PA, Hixson RS, Gray III GT. J Phys Chem Solids 2007;68:2297–302.